ACS APPLIED MATERIALS & INTERFACES

Research Article

www.acsami.org

Tuning the Tribological Property with Thermal Sensitive Microgels for Aqueous Lubrication

Guoqiang Liu,[†,‡] Xiaolong Wang,[†] Feng Zhou,*[,†] and Weimin Liu*[,†]

[†]State Key Laboratory of Solid Lubrication, Lanzhou Institute of Chemical Physics, Chinese Academy of Sciences, Lanzhou 730000, China

[‡]Graduate School of Chinese Academy of Sciences, Beijing 100039, China

ABSTRACT: Thermoresponsive microgels, poly(N-isopropylacrylamide)-graft-poly(ethylene glycol) (PNIPAAm-g-PEG), were synthesized via emulsifier-free emulsion polymerization and the tribological property as water lubricating additive was studied. The microgels had good thermoresponsive collapse/swelling performance with lower critical solution temperature (LCST) ca. 38.4 °C. The rheological characterization and tribological tests showed that the microgels had a good lubricating performance in aqueous lubrication through interfacial physisorption and hydration lubrication, but the friction coefficient was impacted by temperature (below and above LCST). The tunable thermosensitive tribological property was attributed to the hydrophobic interaction and the enhanced interfacial absorption, which were both triggered by the elevated temperature. Furthermore, in order to avoid the water erosion in aqueous lubrication, the microgels were used together with 1H-benzotriazoles (BTA). Because of the good antifriction and anticorrosion property of BTA and the interplay between microgels and BTA, the microgels/BTA exhibited a synergistic effect in aqueous lubrication and the tribological property was more sensitive around the LCST. The present work is beneficial to understanding the tribological property of responsive microgels in aqueous lubrication and provides a novel approach for achieving low-friction through soft matters.

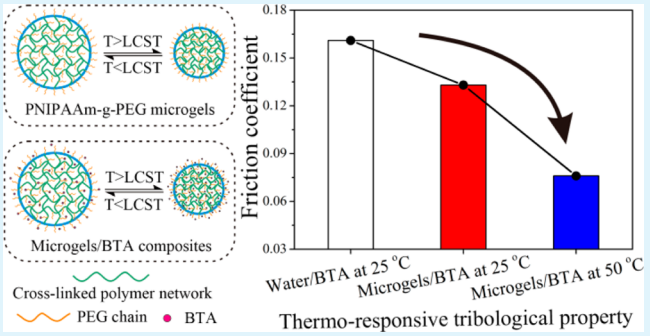

KEYWORDS: *tribology, thermoresponsive, microgels, hydration lubrication, soft matter*

1. INTRODUCTION

Aqueous lubrication is attracting increasing attention in the tribological fields because of the desire to understand and potentially mimic how biotribological contacts lubricate in nature.[1−3] Water is the most common lubricating medium in nature; however, it is only very recently that the friction and lubrication mechanisms was partly disclosed, i.e., the fluidity in confined geometry.[4−6] It is well-known that nonassociating liquids such as organic solvents and oils will turn solid-like with diverged viscosity when confined to just a few monolayers thick between two surfaces sliding past each other, but water, not like the others, keeps persistent fluidity even when confined down to one monolayer.[6] It is believed that water thin films in aqueous media could be considered as hydration layers resulting from the large dipole of water molecule, which are of great significance in terms of lubrication. According to the hydration lubrication mode developed in the past 10 years, the hydration layers formed by polar groups and water molecules have a fluid response to shear, which can not only support high load without being squeezed out but meanwhile remain very rapidly relaxing behavior.[6,7] Although water is a low-cost lubricant with high cooling capability, it is noncompatible for most tribological applications because of the low viscosity and high corrosivity.[8−10] Developing high-performance aqueous lubricant additives is thus becoming an effective and imperative way to improve hydration lubrication.[10]

In nature, soft matters are used to ease sliding of surfaces past each other, so the tribological property of soft matters, including brush-like polymers, colloids, hydrogels, emulsions, surfactants, micelles and suspensions, has become research hotspots recently.[11−14] Hydrogels, which consist of cross-linked hydrophilic polymer networks solvated with water, can exhibit characteristic properties of both solids and liquids.[15] Like solid, their shapes can be changed with stress, whereas like liquid, they allow small size solutes to diffuse through the network. With no doubt, the investigation of friction property of hydrogels is of great importance in revealing the low-friction mechanisms found in biological systems, and thereafter finding novel strategies to develop low-friction soft matters.[15−19]

Microgels are known as cross-linked polymer based micro/nanoparticles that swell only in a good solvent. A particular one of them is stimuli-responsive microgels, which can respond to external stimuli such as temperature, pH, and light.[20] Generally, their responses involve fast and significant volume changes due to the swelling/collapse cycles, or an alteration in the interfacial

Received: July 26, 2013
Accepted: October 11, 2013
Published: October 11, 2013

activity because of hydrophilic/hydrophobic transitions.[20−22] Compared with bulk hydrogels, microgels have larger specific surface area, faster response to external stimuli and better dispersion in aqueous media. Among different kinds of microgels, temperature responsive poly(N-isopropylacrylamide) (PNIPAAm) microgels have attracted exceptional interest because of their unique reversible volume phase transition (VPT) under different temperatures.[23−26] The lower critical solution temperature (LCST) of PNIPAAm is ca. 32 °C. Below LCST, the PNIPAAm microgels are highly swollen, while collapsed at above LCST, resulting in most of the water and dissolved molecule in the gel structure expelled.[26−28] Consequently, the PNIPAAm-based microgels are becoming promising candidates for various applications including drug delivery, biosensors, and responsive interfaces for smart devices.[26,29−33] However, to the best of our knowledge, the research on the frictional/lubrication property of microgels has never been reported yet. Because of good dispersibility in aqueous media, three-dimensional reticular polymer network and excellent collapse/swelling capacity, PNIPAAm-based microgels can be a special kind of soft matter for aqueous lubrication. What's more, one can even expect PNIPAAm-based microgels to achieve a tunable tribological property by controlling the temperature. Poly(ethylene oxide) (PEG), a typical water-soluble polymer[34,35] has shown a promising potential for aqueous lubrication due to its good hydrophilicity and hydration capability.[36,37] In this study, the thermoresponsive PNIPAAm grafted poly(ethylene glycol) methyl ether methacrylate (PNIPAAm-g-PEG) microgels were prepared for tribological research via the emulsifier-free emulsion polymerization.[38,39] The chemical composition was characterized by FTIR, ^{1}H NMR, and TGA. The thermoresponsive property of the microgels, as well as the rheological behavior, was also investigated. Finally, the tribological behavior was evaluated for steel/steel contacts at different temperatures.

It is well-known that the loss caused by steel corrosion is enormous in aqueous lubrication. It is thus of great significance to avoid corrosion of metal friction pairs. To do this, N-substituted benzotriazole compounds have been widely employed, such as 1H-benzotriazoles (BTA), which can not only be an effective anticorrosive additive in aqueous lubrication, but also play an important role in reducing the friction coefficient and wear volume between friction pairs.[40−43] Therefore, PNIPAAm-g-PEG microgels/BTA composites were introduced to improve the aqueous lubricating effect. To compare with the pure microgels, thermoresponsive capability, rheological behavior, and tribological property of the microgels/BTA were investigated systematically too.

2. EXPERIMENTAL SECTION

2.1. Materials. All reagents for microgel synthesis including N-isopropylacrylamide (NIPAAm), poly(ethylene glycol) methyl ether methacrylate (PEGMA, average Mn = 950), N,N′-methylene bis-(acrylamide) (BIS) and the ammonium persulfate (APS) were purchased from Sigma-Aldrich and used as received. 1H-Benzotriazoles (BTA) was obtained from J&K. Deionized water with resistivity of 18.2 MΩ cm at 25 °C was used throughout, which was produced by a Milli-Q water purification system.

2.2. Synthesis of PNIPAAm-g-PEG microgels. The PNIPAAm-g-PEG microgels were prepared via emulsifier-free emulsion polymerization in a similar process as described in our previous works.[38,39] A typical process is as follows: NIPAAm (1.0 g), PEGMA (0.5 g), BIS (0.1 g), and water (60 mL) were added into a 100 mL round-bottom flask equipped with a magnetic stirrer, thermometer, nitrogen inlet and Graham condenser. The mixture was sufficiently mixed with a fine nitrogen flow at room temperature for 30 min before APS (0.075 g) was added into. Next, the polymerization was conducted at 75 °C for 4 h. And finally, the resultant microgel dispersion was put into a dialysis tube with molecular weight cutoff of 8000−14000 to purify for 72 h in 1000 mL of deionized water. The water was changed every 12 h. The concentration of the microgel suspension after dialysis was calculated to be 2.36 wt % by gravimetric analysis, which was then was diluted to 1.0, 1.5, and 2.0 wt % for further use.

2.3. Preparation of PNIPAAm-g-PEG Microgels/BTA Composites. Ten milliliters of 1.0 wt % PNIPAAm-g-PEG microgel aqueous dispersion was put into a round-bottom flask equipped with a magnetic stirrer. Then, 10 mg of BTA was added. The mixture was stirred for 24 h at room temperature in order to enable the BTA molecules to flow freely through the network of microgels to form PNIPAAm-g-PEG microgels/BTA composite.

2.4. Chemical Structure Characterization. FTIR spectrum was obtained on a Perkin-Elmer Transform Infrared Spectrometer (Perkin-Elmer, USA). ^{1}H NMR spectrum was recorded on a UNITY INOVA 600-MHz spectrometer (Varian, USA) using DMSO-d_6 as solvent. The thermal properties of the microgels in air were conducted using a STA 449 C Jupiter simultaneous TG-DSC instrument from room temperature to ∼800 °C with heating rate of 10 °C/min.

2.5. Thermoresponsive Behavior Investigation. The LCST, hydrodynamic diameters (D_h) and particle dispersion index (PDI) of the microgels were investigated. In the first, the transmittance of the colloidal solution (1.0 mg/mL) at 500 nm was recorded using a UV−vis spectrophotometer (Specord-50, Jena, Germany) with a thermostatically controlled cell holder in the range of 20 to 55 °C at heating rate of 0.5 °C/min. The apparatus was calibrated using deionized water. The temperature with half decrease of the total in transmittance was defined as the LCST of microgels. The UV−vis spectrophotometer was also used to study the interaction between microgels and BTA at different temperatures from 25 to 50 °C. Next, the dynamic light scattering technique (DLS) was used to probe the D_h and PDI of microgels from 25 to 55 °C, where a temperature-programmed particle size analyzer (Zetasizer Nano ZS, Malvern Instruments, UK) equipped with a 633 nm He−Ne laser was employed. The swelling ratio (SR) of microgels was calculated using the mean hydrodynamic diameters of microgel particles at 25 and 50 °C (D_{h25} and D_{h50}) according to the equation of $SR = V_{swollen}/V_{shrunken} = (D_{h25}/D_{h50})^3$, where $V_{swollen}$ and $V_{shrunken}$ are the volume of microgel particles at 25 and 50 °C, respectively. Please note that at least 5 min was allowed to reach equilibrium at each temperature for both UV−vis spectrophotometer and DLS measurement.

2.6. Rheological and Tribological Measurement. The rheological property of microgels was investigated using RS6000 Rheometer (Germany). In rheology, tan δ was defined as "dissipation factor", where tan $\delta = G''$ (loss modulus)/G' (storage modulus), which indicates the capability of dissipating energy away from the load-bearing surfaces. The tribological properties of pure microgels and microgels/BTA composites were evaluated on an Optimol SRV-IV oscillating reciprocating friction and wear tester in a ball-on-block configuration, where both the upper running ball and the lower stationary disk are is AISI 52100 steel with 10 and 24 mm in diameter, respectively. The test was conducted for 30 min at 25 and 50 °C, respectively, under the load from 25 to 100 N (frequency, 25 Hz; amplitude, 1 mm). The elastic modulus of steel used in the friction test was 190−210 GPa, and the Hertzian maximum contact pressure was in the range of 1.32−2.10 GPa (from 25 to 100 N). The friction coefficient was the average during the entire 30 min friction test. The wear volume on the lower disk was the mean value of three repetitive measurements on a MicroXAM 3D noncontact surface mapping profiler. X-ray photoelectron spectrometer (XPS) was carried out to characterize the elemental composition using Al Ka radiation. The binding energy was referenced to the C 1s of contaminated carbon at 284.8 eV.

2.7. Interfacial Physisorption. The physisorption of PNIPAAm-g-PEG microgels and PNIPAAm-g-PEG microgels/BTA composites in their swollen and collapsed states on a gold substrate was studied by a

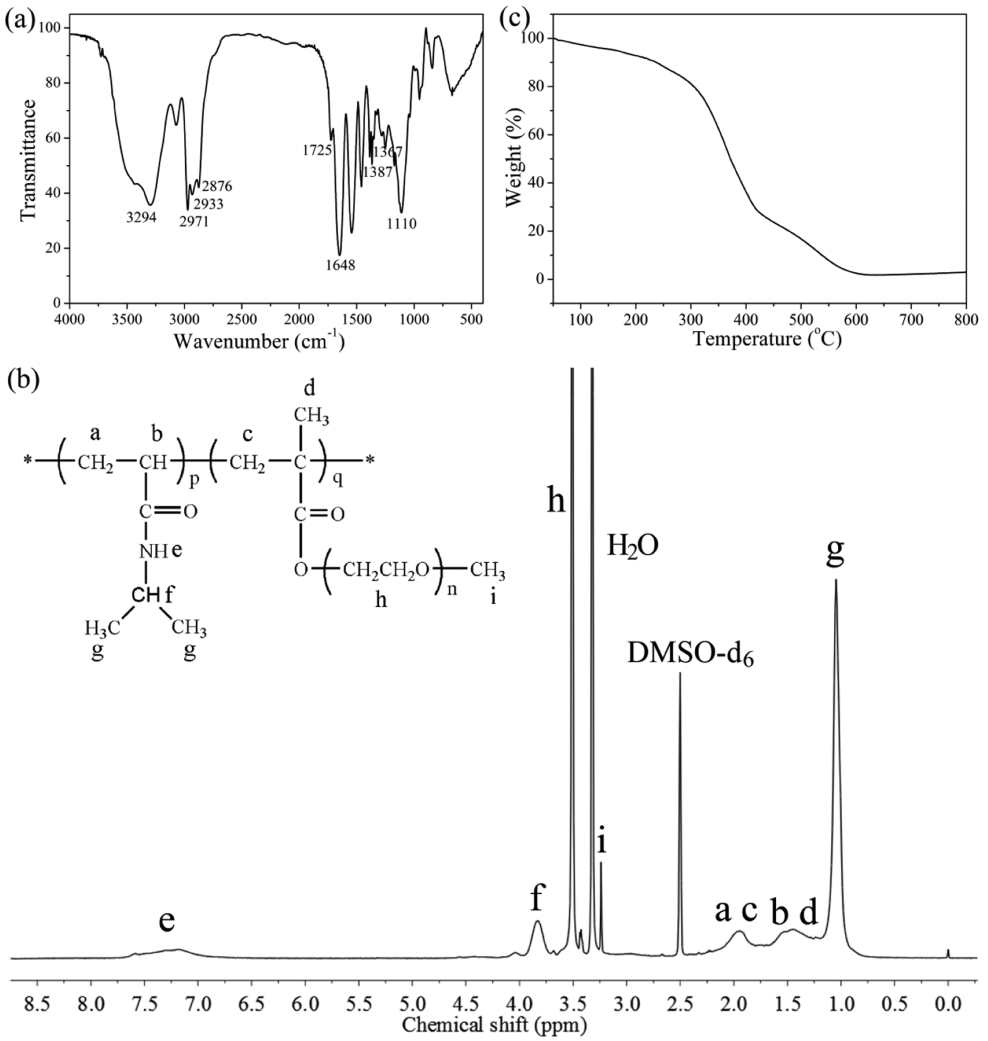

Figure 1. (a) FTIR spectrum of PNIPAAm-g-PEG; (b) ^{1}H NMR spectrum of PNIPAAm-g-PEG; (c) TGA curve of PNIPAAm-g-PEG.

quartz crystal microbalance (E4, Q-Sense, Gothenburg, Sweden) with dissipation (QCM-D) monitoring technique. Deionized water was used for calibration. Precleaned gold coated quartz crystal was employed. In experiment, once the microgel suspension or the microgels/BTA composite suspension filled the flow cell, the real time frequency shift and the dissipation factor change were recorded. Due to the resonant frequency shift ($-\Delta f$) has a positive correlation with the absorption amount on quartz crystal, $-\Delta f$ referred to the water was used to qualitatively present the absorption amount of microgels and microgels/BTA composites. The experiment was performed at 25 and 50 °C, respectively.

3. RESULTS AND DISCUSSION

3.1. Chemical Structure Analysis. First of all, the resultant PNIPAAm-g-PEG microgels were characterized using FTIR, ^{1}H NMR and TGA to investigate its chemical composition and thermal properties. As shown in Figure 1, the chemical structure of the grafted copolymer was well-defined. Figure 1a shows the FTIR spectrum of the microgels, where the appearance of the following signals indicates qualitatively the successful copolymerization of NIPAAm and PEGMA.[38,39] The strong and wide absorption bands at 3600−3200 and 2971−2876 cm^{-1} are attributed to the stretching vibration of N−H groups and C−H in methyl and methylene, respectively. The peaks at 1725 and 1648 cm^{-1} were the characteristic absorption of ester carbonyl and amide carbonyl, respectively. The double peaks at 1387 and 1367 cm^{-1} are assigned to the coupling vibration split absorption of the two methyl groups in $-CH(CH_3)_2$. The strong peak at 1110 cm^{-1} is to the C−O in ether linkage. The ^{1}H NMR spectrum of the copolymer PNIPAAm-g-PEG shown in Figure 1b also confirms its structure, where all the peaks can be accurately identified. Moreover, according to the peak area of the protons in the $-CH(CH_3)_2$ (g, 1.05 ppm) in NIPAAm moiety and $-CH_2CH_2O-$ (g, 3.51 ppm) in PEGMA moiety,[44] the molar ratio of NIPAAm to PEGMA in the copolymer was calculated to be 1.99 to 1, meaning that the PEG content is ca. 33.4% in the copolymer.

The thermal stability of the microgels was evaluated by TGA in air atmosphere. As shown in Figure 1c, the thermo-decomposition temperature of the microgels is ca. 310.6 °C, indicating a good thermodynamic stability. What important is that the thermo decomposition temperature is much higher than the boiling point of water 100 °C, implying that the microgels have no thermal decomposition problem in the process of aqueous lubrication.

3.2. Thermoresponsive Behavior. The thermoresponsive behavior is important for microgels to be used as lubricants. For the present PNIPAAm-g-PEG microgels, the LCST was first measured, and the data are shown in Figure 2. The digital picture embedded in Figure 2a shows the visible phase

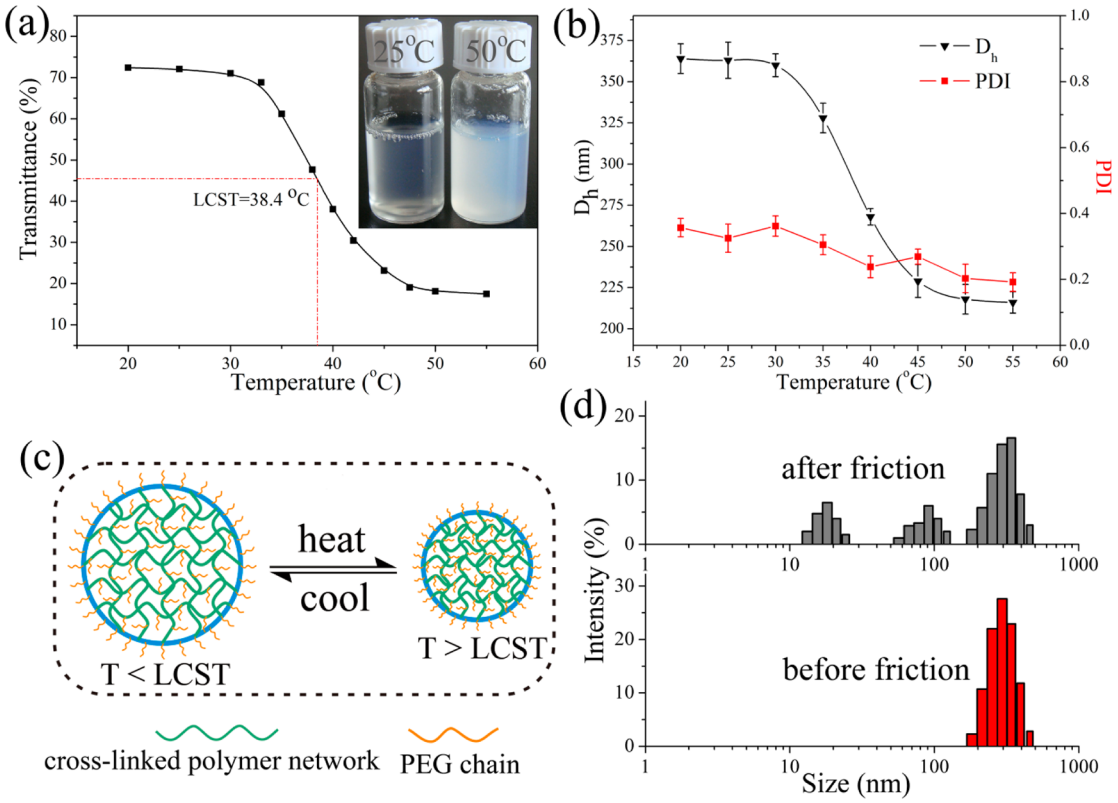

Figure 2. (a) Transmittance of microgel dispersion with temperature at 500 nm; the inset is the digital picture of microgel suspension at 25 and 50 °C. (b) The D_h and PDI of the microgels as a function of temperature; error bar = standard deviation (SD), n = 3 for both D_h and PDI. (c) Schematic diagram illustrating the volume phase transition of PNIPAAm-g-PEG microgels at the LCST. (d) The size distribution of the microgels before and after friction test at 25 °C.

transition. It can be seen that the aqueous microgel dispersion was in close proximity to a transparent solution at 25 °C, whereas transformed into a white turbid emulsion at 50 °C. The transmittance shown in Figure 2a decreased significantly when the temperature was increased from 20 to 55 °C. In our case, the LCST of PNIPAAm-g-PEG microgels was ca. 38.4 °C, at which the transmittance dropped abruptly. According to the literature, the LCST of PNIPAAm shifted to a lower temperature when copolymerized with a hydrophobic comonomer, whereas it shifted to higher temperature with a hydrophilic one.[20,45] This is consistent with the present case; that is, the hydrophilic PEG grafted chains make the LCST higher than that of pure PNIPAAm (ca. 32 °C).

The temperature dependence of D_h of the PNIPAAm-g-PEG microgels in aqueous media was investigated by DLS. As shown in Figure 2b, the D_h of the microgel at 25 °C was ca. 363 nm, whereas at 50 °C it reduced to ca. 218 nm due to the collapse of the microgels. According to the size change during the VPT, the swelling ratio (SR) of the microgel particles is 4.62. This is a crucial parameter indicating the swelling/collapse capacity for microgels. Notably, The PDI values remained lower than 0.4 at the entire temperature range, indicating the narrow size distribution and the uniform collapse behavior of the microgels. In short, the as-prepared microgels exhibited a good thermoresponsive capability.

3.3. Rheological Characterization. To evaluate the microgels as synthetic hydration lubricants, we first assessed their rheological properties. From a rheological perspective, most non-Newtonian fluids and gels may be regarded as soft matters because of their complex response to applied deformation. When a shear rate sweep is performed at incremental of shear stress, soft matter is often found to have a very high viscosity plateau at low shear rates, referred to as the zero-shear viscosity.[41] Above a critical shear rate, extreme shear thinning is observed whereby the viscosity decreases by several orders of magnitude. Figure 3a shows the curves of viscosity versus shear rate of PNIPAAm-g-PEG microgel aqueous suspension (1.5 wt %). It is found that the viscosity decreases gradually with the increasing shear rate, indicating that the microgel suspension can be classified as the non-Newtonian fluid with a shear-thinning property. It is noteworthy that the reduction in viscosity is almost negligible when the shear rate increases to a certain level; beyond that, the microgel suspensions show the characteristic of the Newtonian fluid at a higher shear rate, suggesting a good colloidal and mechanical stability of the microgels in aqueous media. The rheological behaviors of PNIPAAm microgel suspension have been extensively investigated,[46−48] and this type of microgels showed a significant shear-thinning phenomenon, which was not beneficial for aqueous lubrication. After the introduction of PEG chains, the undesired shear-thinning disadvantage was weakened, and the constant high viscosity was helpful to aqueous lubrication.

Figure 3b shows the reversible rheological curve with decreasing shear rate. The as-prepared microgel suspension (1.5%) exhibited a successful reversible transform of viscosity, suggesting a good viscoelasticity. Figure 3c shows the step change of the rheological property. It is found that the viscosity and shear stress of the microgels almost remained constant at a fixed shear rate, indicating that the physical and chemical

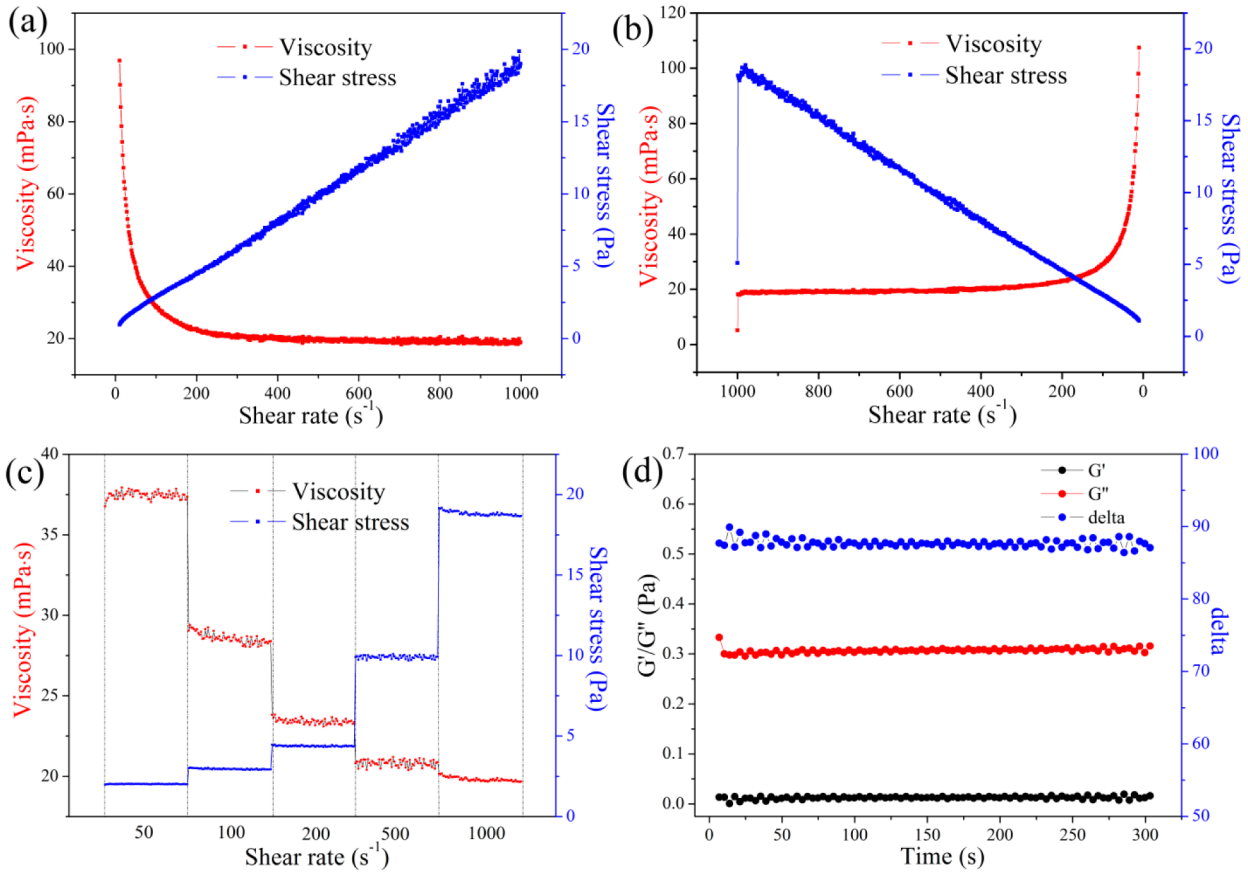

Figure 3. (a) Viscosity versus shear rate curves of the microgel suspension (1.5 wt %). (b) Reversible rheological curve with decreasing the shear rate. (c) Viscosity values and shear stress of microgel suspension (1.5 wt %) at a certain shear rate. (d) Storage moduli (G'), loss moduli (G''), and delta of the microgels suspension (1.5 wt %) as a function of time.

properties of microgels were relatively stable under a certain condition.

The storage modulus G' of soft matter indicates the extent to which the system gives a solid-like response through storage of elastic energy, and the loss modulus G'' characterizes the dissipation, viscous or liquidlike response of the system. Figure 3d shows the plots of storage moduli (G'), loss moduli (G''), and delta of the 1.5 wt % microgels dispersion as a function of time. It is evident that G' and G'' both have the plateau regions of the dynamic moduli and G'' (0.31 Pa) is larger than G' (0.012 Pa) over the entire shear process. The results demonstrate that the microgel suspension was assigned to the viscous fluid that had a characteristic viscous deformation under the shear stress. Consequently, the delta is 87 for the microgel dispersion, revealing that the microgels are able to disperse energy away from the load-bearing surfaces. The rheological values of microgel suspensions at different concentrations are listed in Table 1, where the viiscosity$_{1000}$ refers to the viscosity value at the shear rate of 1000 s^{-1}.

Table 1. Rheological Properties of the Microgel Suspensions (average ± SD; n = 3)

sample	viscosity$_{1000}$ (mPa s)	G' (Pa)	G'' (Pa)	delta
1.0%	8 ± 0.7	0.042 ± 0.002	0.13 ± 0.01	71 ± 1
1.5%	19 ± 0.6	0.012 ± 0.003	0.31 ± 0.01	87 ± 1
2.0%	29 ± 0.8	0.062 ± 0.005	0.53 ± 0.01	83 ± 1

3.4. Tribological Tests of the Microgels. The tribological behavior of the microgel suspension for steel/steel contacts was investigated in a ball-on-block configuration on an Optimol SRV-IV oscillating reciprocating friction and wear tester (constant load, from 25 to 50 N; frequency, 25 Hz; duration, 30 min).[41] The tests were performed at 25 and at 50 °C, respectively. Figure 4a–c shows the friction curves and the averaged wear volumes of the steel discs. At 25 °C, it is notable that the friction coefficients and the averaged wear volumes were both smaller than that of pure water (0.331, 13.61 × 10^{-4} mm^3). Also, as the concentration of the microgel suspension increased, the friction coefficient and the wear volume both decreased gradually. The calculated friction coefficients were 0.208, 0.195, and 0.181, respectively, when the concentration was increased from 1.0 to 1.5 and 2.0 wt %. Besides, compared with that of pure water, the friction curves of the microgel suspensions are relatively stable. These results demonstrate that the PNIPAAm-g-PEG microgels have a good lubricating effect for steel/steel contacts in aqueous lubrication at room temperature. On the one hand, microgels, as a cross-linked polymer, increase the viscosity of water significantly. On the other hand, as a colloid, microgels can absorb onto the surface of friction pairs. More importantly, the three-dimensional network of microgels enable the water molecules to flow freely in the interior of microgels instead of being squeezed out, endowing the microgels with a strong water-holding capacity in the friction process. The plenty of water molecules can form hydration layers with polar groups, which avoid water being squeezed out under large pressure and meanwhile remain very

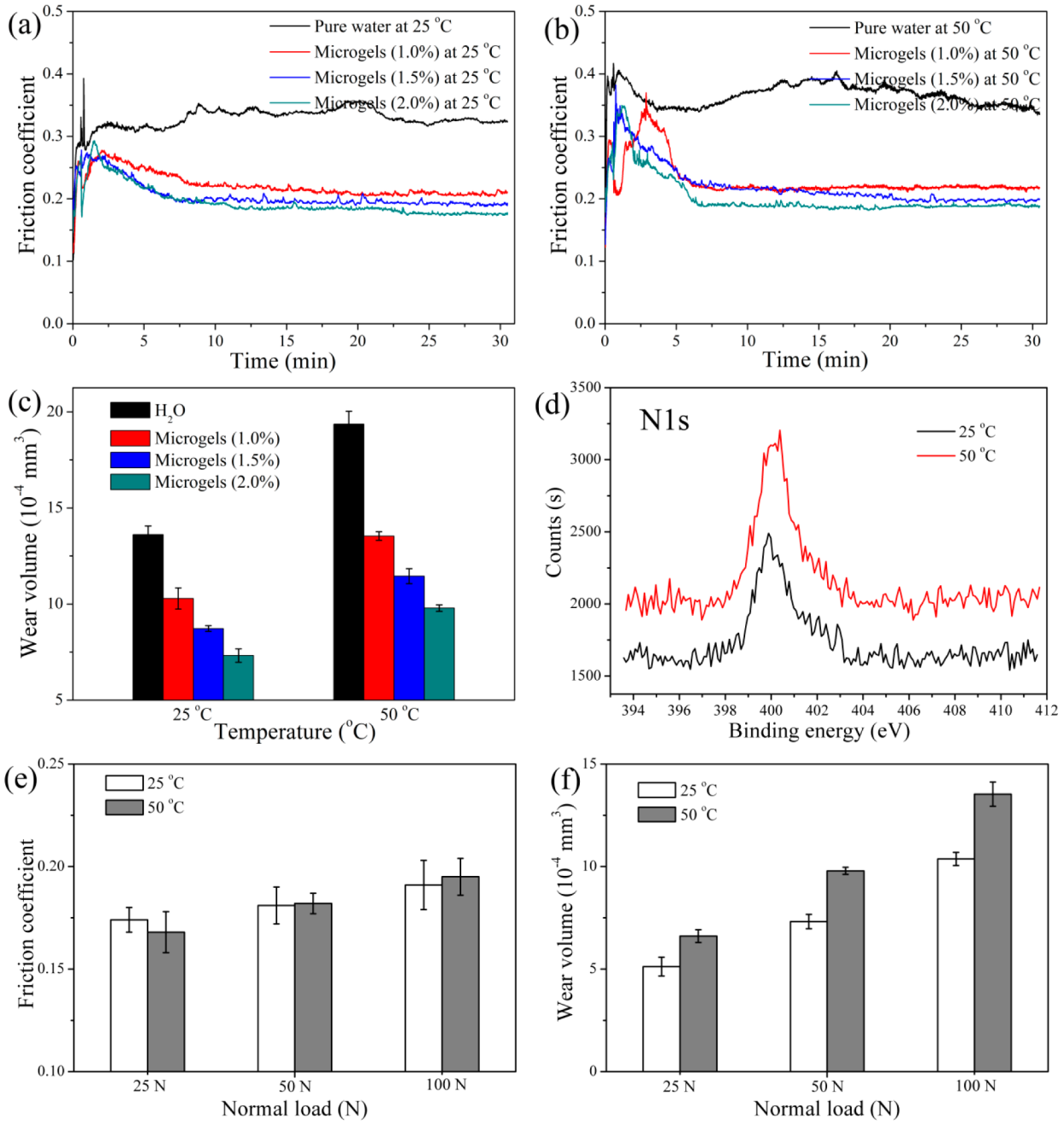

Figure 4. (a) Friction curves of the microgel suspension with different concentrations under the normal load of 50 N at 25 °C. (b) Friction curves of the microgel suspension with different concentrations under the normal load of 50 N at 50 °C. (c) Averaged wear rates from these friction curves. (d) XPS spectra (N1s) of the worn surfaces of steel discs lubricated by 2.0 wt % microgel suspension at 25 and 50 °C. (e, f) Friction coefficients and wear volumes lubricated with 2.0 wt % microgel suspension under different normal load at 25 and 50 °C.

rapidly relaxing and thus exhibit a fluid response to shear. Briefly, the tribological property of the microgels was attributed to the absorption on the interfaces and the hydration layers.

When the temperature was increased to 50 °C, the friction coefficients for steel/steel contacts under the normal load of 50 N did not show obvious change, but the wear volume of steel discs had an increase in comparison with that at 25 °C. The similar friction tests under other normal load of 25 and 100 N was also performed in panels e and f in Figure 4. Under the load of 25 N, the friction coefficient had a slight decrease with the temperature, whereas under the load of 100 N, the friction coefficient increased a bit. Above the LCST, the higher temperature caused the increase of density of the microgels attached to the surface and thereby improved the boundary lubrication, which was confirmed by the XPS spectra (N1s) of the worn steel surfaces in Figure 4d and the subsequent measurement by QCM-D. This factor improved the lubricating effect of microgels. However, increasing the normal load made the deformation of microgels more serious and affected the gel-like state, which decreased the lubricating effect. In short, above the LCST, the two opposite factors led to the different friction coefficients under different normal load.

The increased wear volume was attributed to the phase transition of microgels above the LCST. On the one hand, the phase transition of microgels destroyed the hydration layers, the water in the interior of the microgels was squeezed out, and

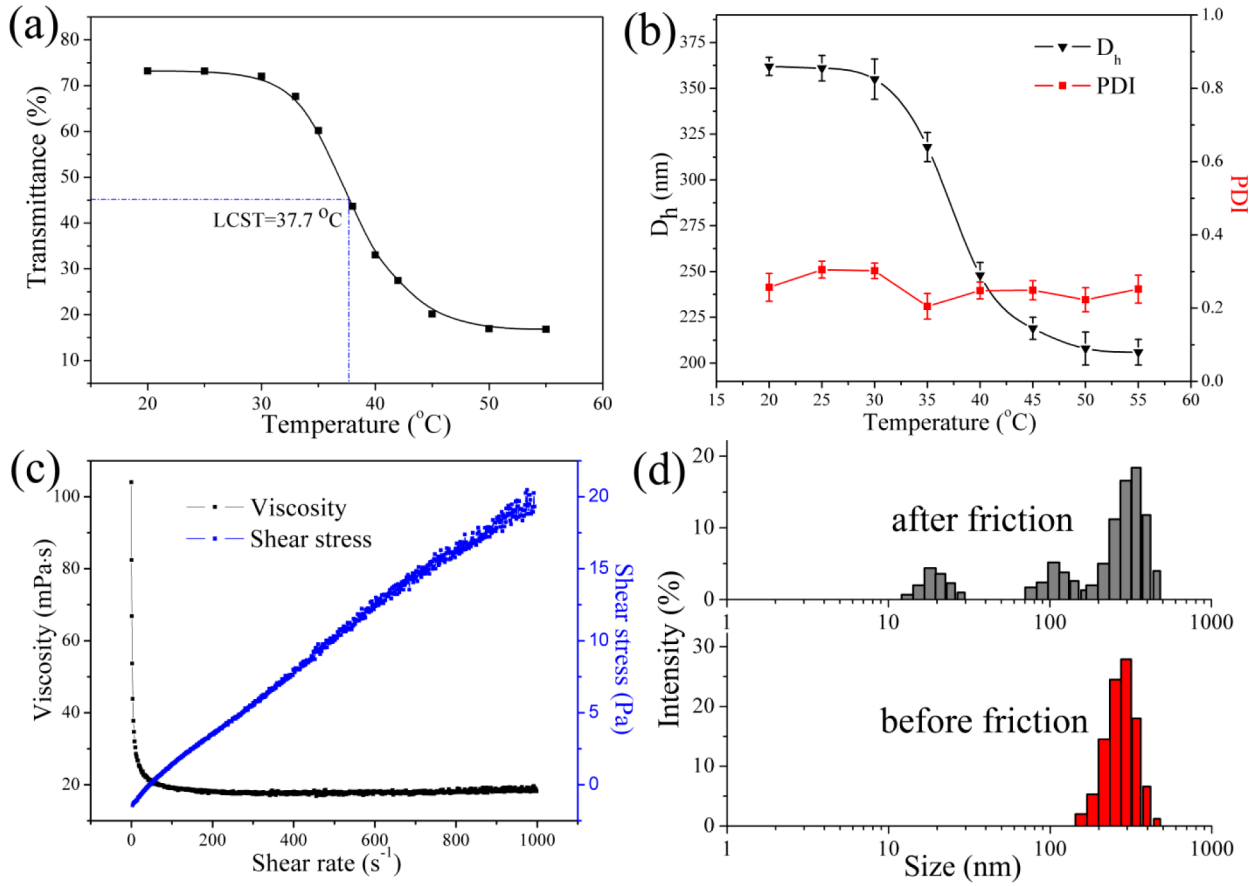

Figure 5. (a) Transmittance change curve of microgels/BTA suspension. (b) D_h and PDI of the microgels/BTA as a function of temperature; error bar = standard deviation (SD), $n = 3$ for both D_h and PDI. (c) Viscosity versus shear rate curves of the microgel suspension ((1.5 wt %)) with BTA (0.2 wt %). (d) Size distribution of the microgels/BTA before and after friction test at 25 °C.

the capability of supporting large pressure was weakened. On the other hand, the partial loss of water-holding capacity water-holding capability increased the water erosion on the steel disc. These two negative factors caused an increase in wear volume of steel disc. In addition, the wear of microgels was investigated by DLS. Figure 2d shows the size distribution of the microgels before and after the friction test. It is found that after the friction tests, some new peaks appeared in the size distribution map, revealing that a portion of microgels has been broken up in the friction process, but importantly, the friction curves were still stable. In brief, compared with pure water, the PNIPAAm-g-PEG microgel suspension achieved a good lubricating effect with reducing friction coefficient and wear volume for steel/steel contacts. Importantly, the as-prepared microgels exhibited a thermoresponsive tribological performance.

3.5. Tribological Tests of Microgels/BTA Composites. In spite of the good antifriction effect, the poor anticorrosion of the microgels based aqueous lubrication is always a big concern for many applications. To overcome this drawback, we further developed a new microgel/BTA composites system, where BTA is a widely used and effective anticorrosive and antifriction additive in aqueous lubrication. It is expected that the microgel/BTA composites could have better tribological properties than the pure microgels.

Before the study of the tribological property, the thermoresponsive capability and the rheological behavior of microgels/BTA were also investigated in comparison with the pure microgels (Figure 5). Panels a and b in Figure 5 show that after the addition of BTA, the microgels still maintained good thermoresponsive capability. Notably, compared with the pure microgels (38.4 °C), the microgels/BTA had a slight decrease in LCST (37.7 °C). Meanwhile, above the LCST, the size of microgels was a little smaller than that of the pure microgels. These differences were attributed to the hydrophobic BTA, which improved the hydrophobicity of microenvironment surrounding the microgel particles. The rheological curve of microgels/BTA suspension (Figure 5c) exhibited an earlier stable stage than that of pure microgel suspension, which was related to the lubricating effect of BTA.

The tribological properties of the microgels/BTA composites (microgels, 1.0, 1.5, and 2.0 wt %; BTA, 0.2 wt %) were investigated by SRV-IV (normal load, from 25 to 50 N, frequency, 25 Hz; duration, 30 min) at 25 and 50 °C, respectively. The 0.2 wt % BTA aqueous solution was employed as reference. Panels a and b in Figure 6 show the friction curves of steel/steel contacts lubricated by the microgels/BTA suspension under the normal load of 50 N at 25 and 50 °C, respectively. Figure 6c shows the averaged wear volumes of steel discs from these friction curves.

When BTA was added into the water, the coefficient (0.161) for steel/steel contacts lubricated by BTA aqueous solution had an apparent decrease compared with that by pure water. Subsequently, after the addition of BTA into the microgel suspension, the friction coefficient and wear volume was also found lower than that by pure microgel suspension at 25 °C. The friction coefficients at 25 °C were calculated to 0.146 (1.0

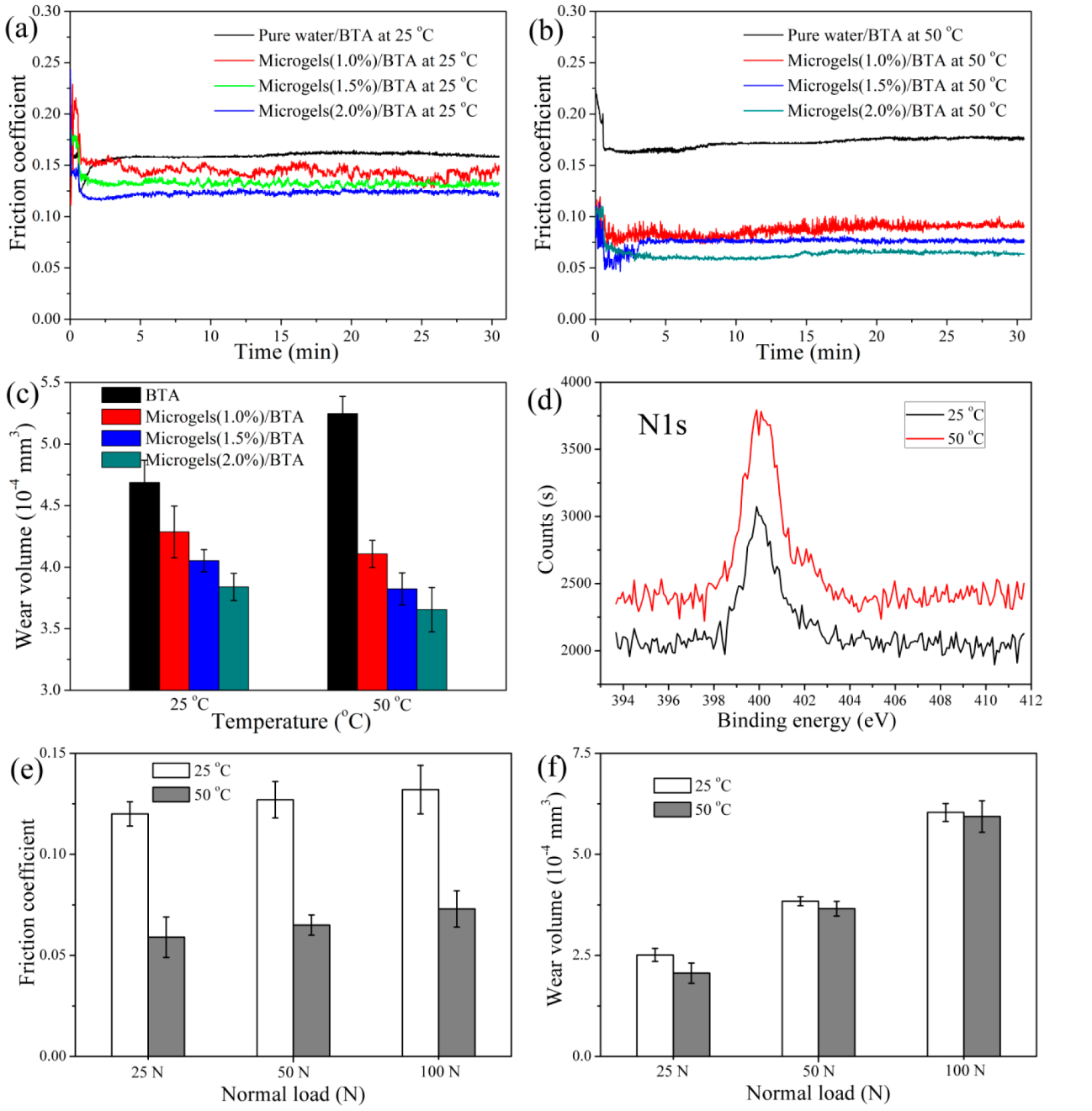

Figure 6. (a) Friction curves of the microgels/BTA composite suspension with different concentrations under the normal load of 50 N at 25 °C. (b) Friction curves of the microgels/BTA composite suspension with different concentrations under the normal load of 50 N at 50 °C. (c) Averaged wear rates from these friction curves. (d) XPS spectra (N1s) of the worn surfaces of steel discs lubricated by microgels/BTA suspension at 25 and 50 °C. (e) Friction coefficients with microgels/BTA suspension (microgels, 2.0 wt %; BTA, 0.2 wt %) under different normal load at 25 and 50 °C. (f) Wear volumes microgel/BTA suspension (microgels, 2.0 wt %; BTA, 0.2 wt %) under different normal load at 25 and 50 °C.

wt %), 0.133 (1.5 wt %), and 0.127 (2.0 wt %). Interestingly, when the temperature was increased to 50 °C, the friction coefficient decreased sharply, and had a gradual further decrease with the concentration of microgels, so as to the wear volume. The friction coefficient for the microgels/BTA composites decreased sharply to 0.091 (1.0 wt %), 0.076 (1.5 wt %), and 0.065 (2.0 wt %) at 50 °C, respectively. The friction tests under normal load of 25 and 100 N were also performed as shown in panels e and f in Figure 6. Similar variations were observed. When the temperature was increased above the LCST, the thermal breakage of the hydrogen bonds enabled the strong hydrophobic interaction between BTA and the hydrophobic segments of the microgel polymers. Importantly, the higher temperature increased the density of microgels attached to the surface, and thereby improved the boundary lubrication due to the increased absorption. Meanwhile, the hydrophobic interaction increases the amount of BTA carried by microgels, so the absorption of microgels and BTA at interface were both improved, which was confirmed by XPS spectra (N1s) of the worn steel surfaces (Figure 6d) and the subsequent QCM measurement. Because of the good antifriction property, the increased absorption of microgels/BTA at frictional surfaces resulted in a better lubricating effect than that of the pure microgels. Besides, the wear of microgels/BTA was also

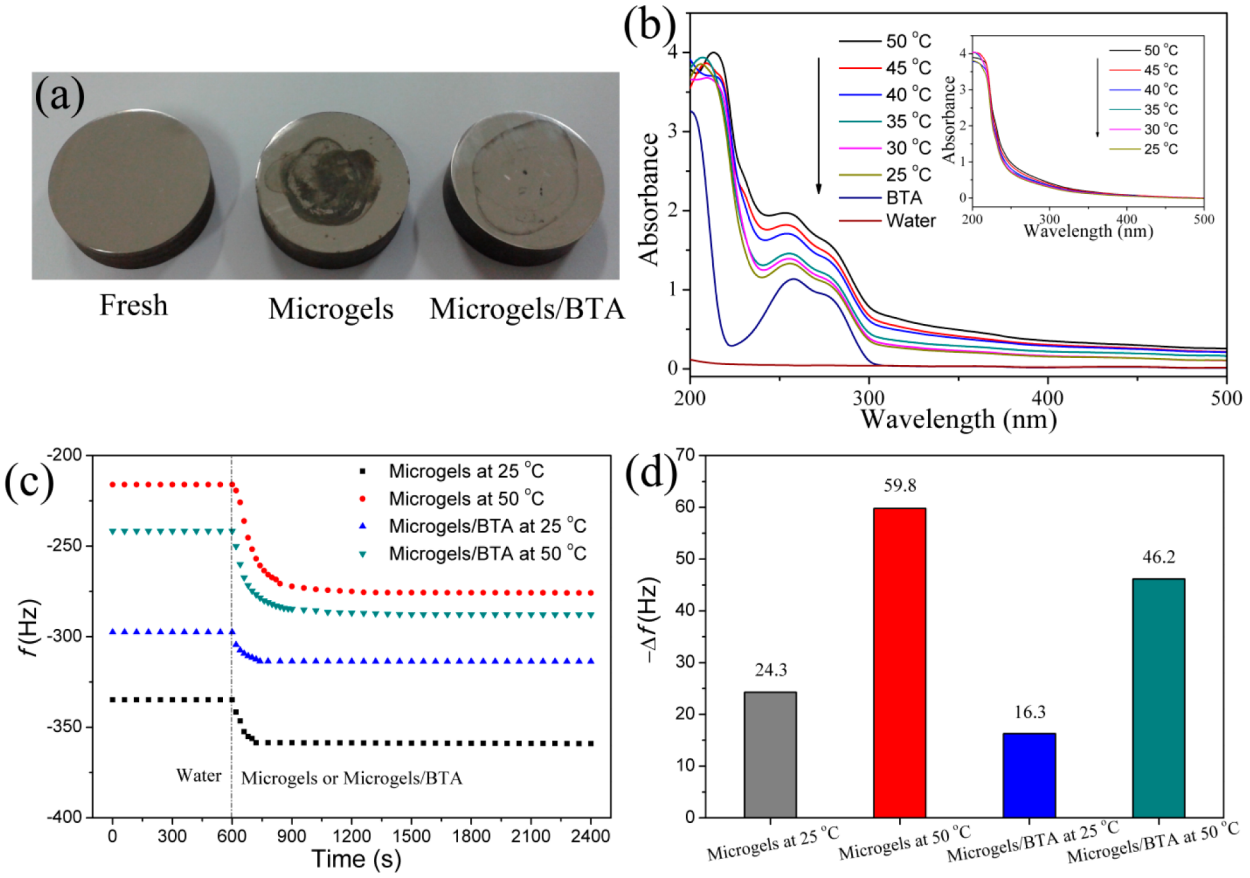

Figure 7. (a) Digital pictures of steel blocks after 6 cycling runs of friction test. (b) UV−vis spectra of microgels/BTA aqueous suspensions (microgels, 0.5 mg/mL; BTA, 0.1 mg/mL) at different temperatures. UV−vis spectra of pure microgels were in an inset. (c) Plots for the time dependence of the resonant frequency (f) of the QCM-D after the addition of the microgels and the microgels/BTA composites (microgels, 0.5 mg/mL; BTA, 0.1 mg/mL) at 25 and 50 °C. (d) Resonance frequency shift ($-\Delta f$) using the water as the reference.

investigated by measuring the size distribution before and after friction tests as shown in Figure 5d. It is found that the amount of broken microgels had a slight decrease in comparison with the previous lubricating system using pure microgels.

Unlike pure microgels, an obvious anticorrosion was also realized with the microgels/BTA composites. As shown in Figure 7a, after 6 runs of friction tests, the color of steel block did not exhibit significant change in comparison with the fresh steel block. Because of the good antifriction and anticorrosion property of BTA, the microgels/BTA played a more significant role than pure microgels in aqueous lubrication.

3.6. Interfacial Physisorption Characterization. To further understand the effect of temperature on the tribological property, we conducted UV−vis spectroscopy and interfacial physisorption characterization. Figure 7b shows the UV−vis spectra of microgels/BTA composite aqueous suspensions at different temperatures. For pure BTA aqueous solution, there is a characteristic UV absorption peak at the wavelength of 257 nm. As the inset shows, the pure microgels suspension had no absorption peak at 257 nm from 25 to 50 °C. When the microgels were added into the BTA aqueous solution, the UV absorption intensity of BTA increased, and the absorption peak exhibited a slight blue shift. Importantly, when the temperature was increased from 25 to 50 °C, the UV absorption intensity of BTA had a marked gradual increase. Especially when the temperature was in the range of 35 to 40 °C, just cross the LCST, an abrupt UV absorption increase happened. These results reveal that the VPT enhanced the interaction between BTA and the microgels. When the hydrogen bonds were broken above the LCST, the hydrophobic BTA molecules got stronger interaction with the hydrophobic segments of the microgel polymers, which increased the concentration of BTA molecules in the interior of microgels. Consequently, the amount of BTA carried by microgels above the LCST is larger than that below the LCST, leading to a mutual increase of microgels and BTA attached to the surfaces at higher temperate.

Except for the hydrated lubrication, the other important contribution for the friction of adhesive gels is surface absorption. Therefore, the physisorption property of PNIPAAm-g-PEG microgels and PNIPAAm-g-PEG microgels/BTA composites in their swollen and collapsed states on a gold substrate was studied by a quartz crystal microbalance with dissipation (QCM-D), as showin in panels c and d in Figure 7. In Figure 7c, the plot in the first 600 s displays the physisorption equilibrium of deionized water, and that in the next 1800 s is the physisorption process of the microgels and microgels/BTA composites. It is found that after the addition of microgels or microgels/BTA composites, the f decreased significantly, suggesting a marked physisorption on the quartz crystal. In Figure 7d, it is clear that the Δf of microgels at 25 °C (in swollen state) was much smaller than that at 50 °C (in collapse state). The VPT of microgels led the collapse of microgels, suggesting a more compact arrangement of microgels on the substrate, even a multilayer absorption.[49,50] Meanwhile, in spite of the VPT at the LCST, PEG-grafted

chains still enabled the good hydrophilicity of the outer layer of microgels. These factors indicate that the physisorption mass of the microgels in collapse state is much larger than that in the swollen state. Correspondingly, the physisorption mass of the microgels/BTA composites at 50 °C is much larger than that at 25 °C, too. In addition, the Δf of microgels/BTA composites is a litter smaller than that of pure microgels at both 25 and 50 °C, which may be attributed to the hydrophobicity of BTA.

4. CONCLUSIONS AND PERSPECTIVES

In summary, the thermoresponsive PNIPAAm-g-PEG microgels were successfully synthesized and exhibited good collapse/swelling property in response to the medium temperature. Rheological characterization indicated that the microgels had good colloidal stability during the long high-speed shearing process. Tribological tests showed that the microgels possessed a good lubricating effect in aqueous lubrication, and exhibited a thermosensitive tribological property. When composited with BTA, the microgels/BTA composites showed both antifriction and anticorrosion performance. More importantly, the tribological property was tunable by controlling the temperature, which was attributed to the hydrophobic interaction and the enhanced interfacial absorption. This tunable thermosensitive tribological property in aqueous lubrication may lead to new strategies to develop highly efficient aqueous lubrication systems for biological and biomedical applications, especially in lubricating artificial implanted metal joints.

AUTHOR INFORMATION

Corresponding Authors

*E-mail: zhouf@licp.cas.cn.

*E-mail: wmliu@licp.cas.cn.

Notes

The authors declare no competing financial interest.

ACKNOWLEDGMENTS

The authors acknowledge the financial support from the NSFC (21125316, 51171202), 973 project (2013CB632300), and Key Research Program of the Chinese Academy of Sciences (KJZD-EW-M01).

REFERENCES

(1) Wathier, M.; Lakin, B. A.; Bansal, P. N.; Stoddart, S. S.; Snyder, B. D.; Grinstaff, M. W. *J. Am. Chem. Soc.* **2013**, *135*, 4930−4933.
(2) Kyomoto, M.; Moro, T.; Saiga, K.; Hashimoto, M.; Ito, H.; Kawaguchi, H.; Takatori, Y.; Ishihara, K. *Biomaterials* **2012**, *33*, 4451−4459.
(3) Stokes, J. R.; Macakova, L.; Chojnicka-Paszun, A.; de Kruif, C. G.; de Jongh, H. H. J. *Langmuir* **2011**, *27*, 3474−3484.
(4) Raviv, U.; Laurat, P.; Klein, J. *Nature* **2001**, *413*, 51−54.
(5) Raviv, U.; Perkin, S.; Laurat, P.; Klein, J. *Langmuir* **2004**, *20*, 5322−5332.
(6) Klein, J. *Friction* **2013**, *1*, 1−23.
(7) Briscoe, W. H.; Titmuss, S.; Tiberg, F.; Thomas, R. K.; McGillivray, D. J.; Klein, J. *Nature* **2006**, *444*, 191−194.
(8) Coles, J. M.; Chang, D. P.; Zauscher, S. *Curr. Opin. Colloid Inerfiace Sci.* **2010**, *15*, 406−416.
(9) Zhang, C. H.; Liu, J. M.; Zhang, C. H.; Liu, S. S. *Wear* **2012**, *292*, 11−16.
(10) Zhang, C. L.; Zhang, S. M.; Yu, L. G.; Zhang, Z. J.; Wu, Z. S.; Zhang, P. Y. *Appl. Surf. Sci.* **2012**, *259*, 824−830.
(11) Spirin, L.; Galuschko, A.; Kreer, T.; Binder, K.; Baschnagel, J. *Phys. Rev. Lett.* **2011**, *106*, 168301−168304.
(12) Dedinaite, A.; Pettersson, T.; Mohanty, B.; Claesson, P. M. *Soft Matter* **2010**, *6*, 1520−1526.
(13) Tadmor, R.; Janik, J.; Klein, J.; Fetters, L. J. *Phys. Rev. Lett.* **2003**, *91*, 115503−115506.
(14) Dėdinaitė, A. *Soft Matter* **2012**, *8*, 273−284.
(15) Gong, J. P.; Du, M., Surface Friction and Lubrication of Polymer Gels. In *Surfactants in Tribology*; CRC Press: Boca Raton, FL, 2008; Vol. *1*.
(16) Freeman, M. E.; Furey, M. J.; Love, B. J.; Hampton, J. M. *Wear* **2000**, *241*, 129−135.
(17) Gong, J. P. *Soft Matter* **2006**, *2*, 544−552.
(18) Oogaki, S.; Kagata, G.; Kurokawa, T.; Kuroda, S.; Osada, Y.; Gong, J. P. *Soft Matter* **2009**, *5*, 1879−1887.
(19) Katta, J. K.; Marcolongo, M.; Lowman, A.; Mansmann, K. A. *J. Biomed. Mater. Res. A* **2007**, *83A*, 471−479.
(20) Liu, G.; Zhu, C.; Xu, J.; Xin, Y.; Yang, T.; Li, J.; Shi, L.; Guo, Z.; Liu, W. *Colloids Surf., B* **2013**, *111C*, 7−14.
(21) Parasuraman, D.; Serpe, M. J. *ACS Appl. Mater. Interfaces* **2011**, *3*, 4714−4721.
(22) Wang, Q. C.; Uzunoglu, E.; Wu, Y.; Libera, M. *ACS Appl. Mater. Interfaces* **2012**, *4*, 2498−2506.
(23) Wu, T.; Zou, G.; Hu, J. M.; Liu, S. Y. *Chem. Mater.* **2009**, *21*, 3788−3798.
(24) Wei, H.; Cheng, S. X.; Zhang, X. Z.; Zhuo, R. X. *Prog. Polym. Sci.* **2009**, *34*, 893−910.
(25) Yusa, S.; Yamago, S.; Sugahara, M.; Morikawa, S.; Yamamoto, T.; Morishima, Y. *Macromolecules* **2007**, *40*, 5907−5915.
(26) Acciaro, R.; Gilanyi, T.; Varga, I. *Langmuir* **2011**, *27*, 7917−7925.
(27) Chaudhuri, R. G.; Paria, S. *Chem. Rev.* **2012**, *112*, 2373−2433.
(28) Zhao, C. Z.; Yuan, G. C.; Han, C. C. *Macromolecules* **2012**, *45*, 9468−9474.
(29) Wong, J. E.; Richtering, W. *Curr. Opin. Colloid Interface Sci.* **2008**, *13*, 403−412.
(30) Hu, L.; Serpe, M. J. *Chem. Commun.* **2013**, *49*, 2649−2651.
(31) Islam, M. R.; Serpe, M. J. *Macromolecules* **2013**, *46*, 1599−1606.
(32) Motornov, M.; Roiter, Y.; Tokarev, I.; Minko, S. *Prog. Polym. Sci.* **2010**, *35*, 174−211.
(33) Ngai, T.; Auweter, H.; Behrens, S. H. *Macromolecules* **2006**, *39*, 8171−8177.
(34) Weber, C.; Hoogenboom, R.; Schubert, U. S. *Prog. Polym. Sci.* **2012**, *37*, 686−714.
(35) Mangold, C.; Wurm, F.; Obermeier, B.; Frey, H. *Macromolecules* **2010**, *43*, 8511−8518.
(36) Lee, S.; Muller, M.; Ratoi-Salagean, M.; Voros, J.; Pasche, S.; De Paul, S. M.; Spikes, H. A.; Textor, M.; Spencer, N. D. *Tribol. Lett.* **2003**, *15*, 231−239.
(37) Heeb, R.; Lee, S.; Venkataraman, N. V.; Spencer, N. D. *ACS Appl. Mater. Interfaces* **2009**, *1*, 1105−1112.
(38) Liu, G.; Li, X.; Xiong, S.; Li, L.; Chu, P. K.; Wu, S.; Xu, Z. *J. Fluor. Chem.* **2012**, *135*, 75−82.
(39) Liu, G.; Li, X.; Xiong, S.; Li, L.; Chu, P. K.; Yeung, K. W. K.; Wu, S.; Xu, Z. *Colloid Polym. Sci.* **2011**, *290*, 349−357.
(40) Cai, M.; Liang, Y.; Yao, M.; Xia, Y.; Zhou, F.; Liu, W. *ACS Appl. Mater. Interfaces* **2010**, *2*, 870−876.
(41) Cai, M.; Liang, Y.; Zhou, F.; Liu, W. *ACS Appl. Mater. Interfaces* **2011**, *3*, 4580−4592.
(42) Cai, M. R.; Liang, Y. M.; Zhou, F.; Liu, W. M. *J. Mater. Chem.* **2011**, *21*, 13399−13405.
(43) Zhu, J. M.; Chu, R. Z.; Meng, X. L. *Lubr. Sci.* **2009**, *21*, 103−109.
(44) Li, P.; Xu, R.; Wang, W.; Li, X.; Xu, Z.; Yeung, K. W.; Chu, P. K. *Colloids Surf., B* **2013**, *101*, 251−255.
(45) Park, J. S.; Kataoka, K. *Macromolecules* **2006**, *39*, 6622−6630.
(46) Senff, H.; Richtering, W.; Norhausen, C.; Weiss, A.; Ballauff, M. *Langmuir* **1999**, *15*, 102−106.
(47) Stieger, M.; Pedersen, J. S.; Lindner, P.; Richtering, W. *Langmuir* **2004**, *20*, 7283−7292.
(48) Berndt, I.; Richtering, W. *Macromolecules* **2003**, *36*, 8780−8785.

(49) Wang, P.; Fang, J. J.; Hou, Y.; Du, X. B.; Zhu, D. M. *J. Phys. Chem. C* **2009**, *113*, 729−735.
(50) Wu, K.; Wu, B.; Wang, P.; Hou, Y.; Zhang, G. Z.; Zhu, D. M. *J. Phys. Chem. B* **2007**, *111*, 8723−8727.